THE JOURNAL OF PHYSICAL CHEMISTRY C

Article

Cite This: J. Phys. Chem. C XXXX, XXX, XXX−XXX

pubs.acs.org/JPCC

Understanding Methanol Coupling on $SrTiO_3$ from First Principles

Runhong Huang,[†] Victor Fung,[†] Yafen Zhang,[‡] David R. Mullins,[‡] Zili Wu,[‡,§] and De-en Jiang*[,†]

[†]Department of Chemistry, University of California, Riverside, California 92521, United States

[‡]Chemical Sciences Division, Oak Ridge National Laboratory, Oak Ridge, Tennessee 37831, United States

[§]Center for Nanophase Materials Sciences, Oak Ridge National Laboratory, Oak Ridge, Tennessee 37831, United States

Supporting Information

ABSTRACT: Perovskites are interesting materials for catalysis due to their great tunability. However, the correlation of many reaction processes to the termination of a perovskite surface is still unclear. In this study, we use the methanol coupling reaction on the $SrTiO_3$(100) surface as a probe reaction to investigate direct C−C coupling from a computational perspective. We use density functional theory to assess methanol adsorption, C−H activation, and direct C−C coupling reactions on the $SrTiO_3$(100) surface of different terminations. We find that, although methanol molecules dissociatively adsorb on both A and B terminations with similar strength, the dehydrogenation and C−C coupling reactions have significantly lower activation energies on the B termination than on the A termination. The predicted formation of methoxy and acetate on the $SrTiO_3$(100) B termination can well explain the ambient-pressure XPS data of methanol on the single-crystal $SrTiO_3$(100) surface at 250 °C. This work suggests that a choice of B termination of perovskites would be beneficial for the C−C coupling reaction of methanol.

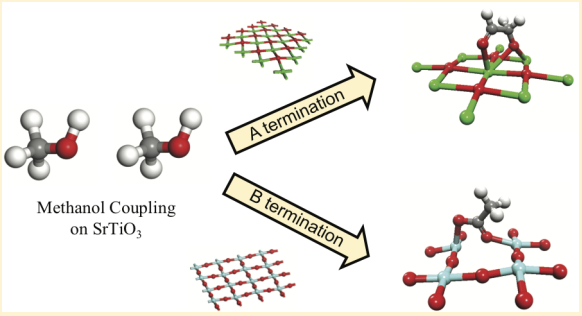

1. INTRODUCTION

C−C coupling reactions are of great importance in both fundamental chemistry and commercial processes.[1−3] For example, they are practiced in chemical industry,[4] where methanol is used as a cheap and abundant feedstock for chemicals via the methanol-to-olefin (MTO) process[3,5,6] and for fuel through the methanol-to-gasoline (MTG) process.[2,7,8]

The coupling reactions have been commonly realized in zeolite catalysts[2,3,9−11] and on transition metals[12−15] but less on transition-metal oxide or perovskite surfaces. It is therefore interesting to examine how oxygenates such as methanol couple on perovskite surfaces. Perovskite-type materials represent a promising class of metal-oxide catalysts, exhibiting superior thermal stability, chemical tunability, redox properties, and acid−base behavior.[8,16−19] They have a general formula of ABO_3, with the A cation being lanthanide, alkaline, or alkaline-earth elements and B usually being a transition metal element.[17] One of the great advantages of perovskites is its compositional variability.[18,19] The composition can be easily tuned by partially substituting A or B cations by other elements.[17] This compositional variation gives rise to a great flexibility in perovskite electronic structures, which in turn affects perovskite catalytic activities.[17,20,21]

Perovskites have been used for oxidative coupling of methane (OCM).[22,23] For example, lanthanum-based perovskite catalysts are reported to have high OCM activities because of the high surface basicity as well as high electron and ion mobility.[23] Borchert et al. reported that $LaAlO_3$ has superior OCM catalytic activities.[22] Moreover, promotion with alkaline metal ions, such as Na or K, helps form oxygen vacancies in perovskites and further improves catalytic activities.[24]

In contrast with the numerous studies of OCM on perovskites, coupling of oxygenates on perovskites has rarely been explored. Recently, it was observed that adsorbed methanol molecules can undergo coupling reactions and form acetate species on $SrTiO_3$ surfaces.[25] However, the underlying mechanisms are not well understood. To this end, here we employ density functional theory to investigate methanol adsorption and reaction on a typical $SrTiO_3$(100) surface; we especially focus on C−C coupling reactions. This work aims to understand how oxygenate molecules couple on a perovskite surface and correlate the reactivity to the surface termination, thereby laying a foundation for further exploration of oxygenate chemistry on perovskite surfaces.

2. COMPUTATIONAL AND EXPERIMENTAL METHODS

Density functional theory calculations were performed by using the Vienna *ab initio* simulation package (VASP)[26] with periodic boundary conditions. The Perdew−Burke−Ernzerhof (PBE) functional was employed to describe electron exchange and correlation.[27] The projector augmented wave (PAW) method was used to describe the interaction between the core and the valence electrons.[28,29] A kinetic energy cutoff of 450 eV was used for the plane waves, and all of the calculations were spin-

Received: January 9, 2018
Revised: March 7, 2018
Published: March 19, 2018

DOI: 10.1021/acs.jpcc.8b00273
J. Phys. Chem. C XXXX, XXX, XXX−XXX

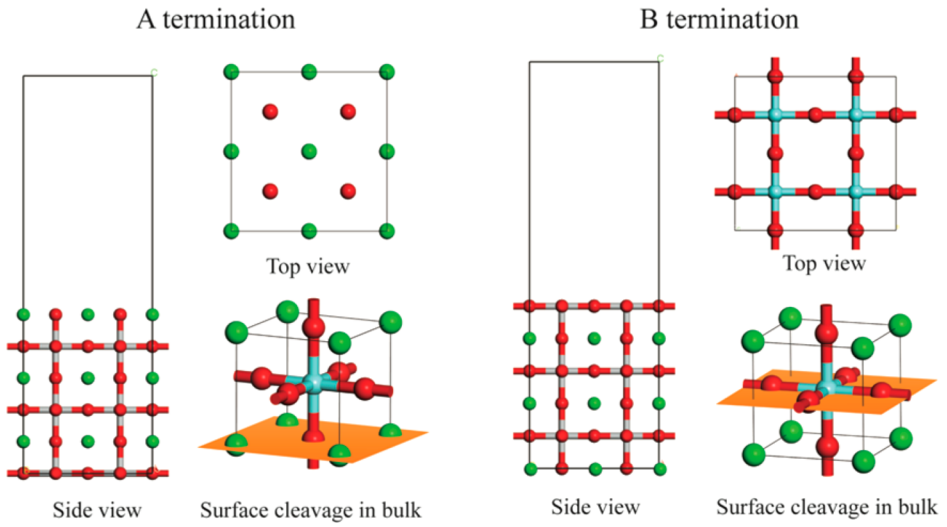

Figure 1. Atomistic models of the $SrTiO_3(100)$ surface of A termination and B termination. Color code: Sr, green; Ti, cyan; O, red.

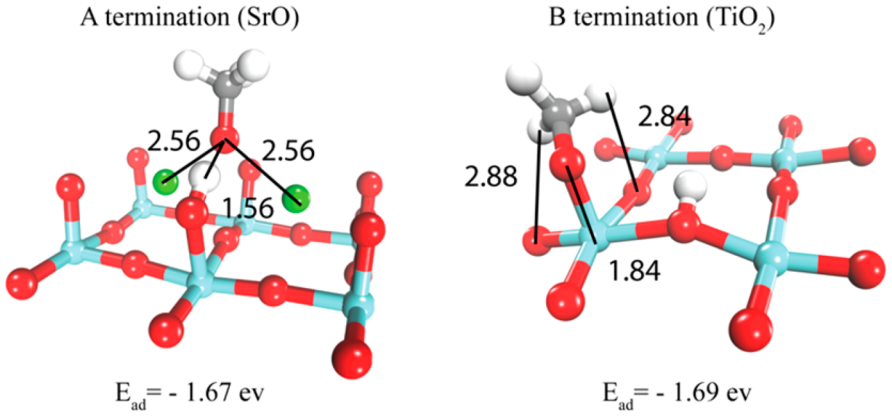

Figure 2. Dissociative methanol adsorption on the $SrTiO_3(100)$ surface's A termination and B termination. Key distances are given in Å. Color code: Sr, green; Ti, cyan; O, red; C, gray; H, white. Only the surface layer is shown.

polarized. Structure relaxation was achieved by optimizing all ionic positions until the force was less than 0.01 eV/Å. The DFT-optimized lattice parameter of single-crystal $SrTiO_3$ (STO) is 3.985 Å, in good agreement with the experiment value (a = 3.905 Å).[30]

We employed the (2 × 2) supercell of the (100) surface of $SrTiO_3$. A vacuum space of 15 Å was created in the z direction to avoid interactions between slabs. The STO(100) surface was constructed by stacking six atomic layers of alternating compositions of SrO and TiO_2. The Brillouin zone was sampled using a 3 × 3 × 1 Monkhorst–Pack scheme. The DFT-D3 method was employed for van der Waals corrections of methanol adsorption and coupling.[31] Climbing-image nudged-elastic-band (CI-NEB) calculations were performed to find the minimum-energy pathways,[32,33] with a force criterion of 0.05 eV/Å. The adsorption energy was calculated as $E_{ad} = E_{surface+adsorbate} - E_{surface} - E_{adsorbate}$, where $E_{surface+adsorbate}$, $E_{surface}$, and $E_{adsorbate}$ denote the energies of the perovskite slab with the adsorbate, the clean slab, and an isolated adsorbate, respectively.

We chose the (2 × 2) supercell for two reasons: (i) from the experimental perspective, the ambient-pressure X-ray photoelectron spectroscopy (see below) was performed at 0.1 Torr of methanol, which would likely lead to relatively high coverages of methanol and its reaction products on the surface; (ii) from the computational perspective, transition-state search is expensive and a smaller cell would allow us to explore many possible pathways. We tested the energetics of methanol dissociative adsorption on the A and B terminations for a larger (3 × 3) supercell and found an uncertainty of 0.1–0.2 eV, which is comparable to usual DFT uncertainties in energetics. Thus, given these considerations, we think that the (2 × 2) supercell is a reasonable choice.

To compare our DFT results with the experiment, the ambient-pressure X-ray photoelectron spectroscopy (APXPS) data of methanol on a single-crystal $SrTiO_3(100)$ surface were also shown. APXPS was performed at Beamline 23-ID-2 (CSX-2) at the National Synchrotron Light Source II (NSLS II) at Brookhaven National Laboratory. A single-crystal $SrTiO_3(100)$ surface was purchased from MTI Corporation and was oxidized in the presence of 0.02 Torr of O_2 at 500 °C until no carbon was detected and Ti was fully oxidized. Methanol was degassed by several freeze–pump–thaw cycles and dosed onto the surface at 0.1 Torr by backfilling through a leak valve to the APXPS chamber. Other experimental details can be found in ref 25.

3. RESULTS AND DISCUSSION

For perovskites, the (100) surface is the most commonly exposed facet. We focused on the (100) surface because it is

DOI: 10.1021/acs.jpcc.8b00273
J. Phys. Chem. C XXXX, XXX, XXX–XXX

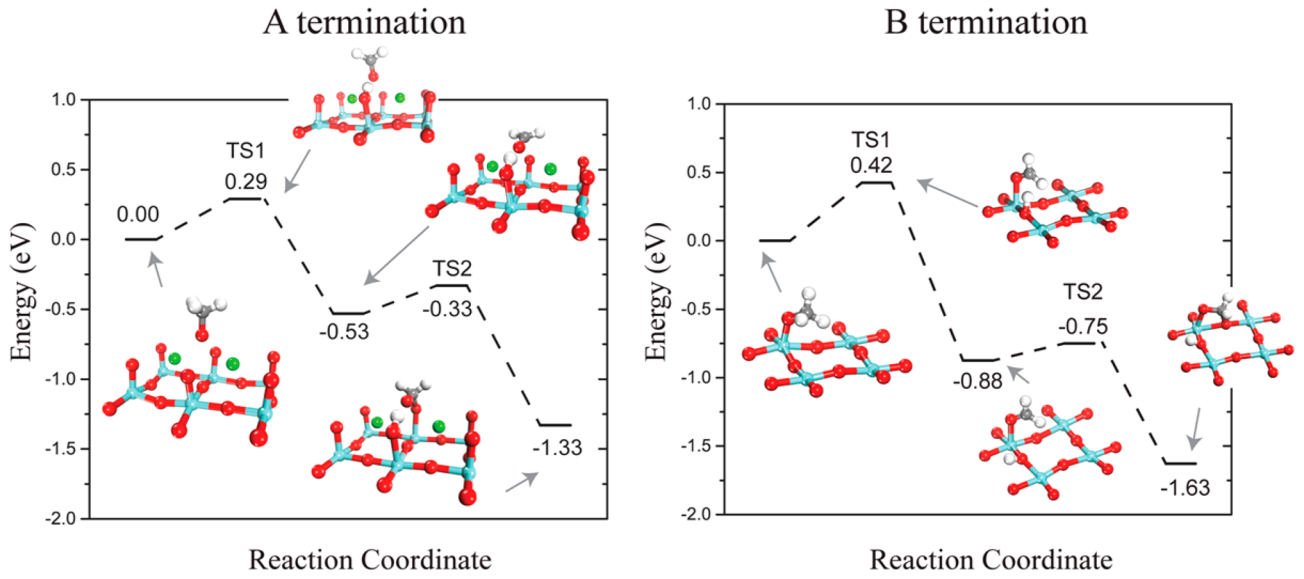

Figure 3. First C−H bond activation of methoxy on $SrTiO_3(100)$ of A termination and B termination. Color code: Sr, green; Ti, cyan; O, red; C, gray; H, white. Only the surface layer is shown.

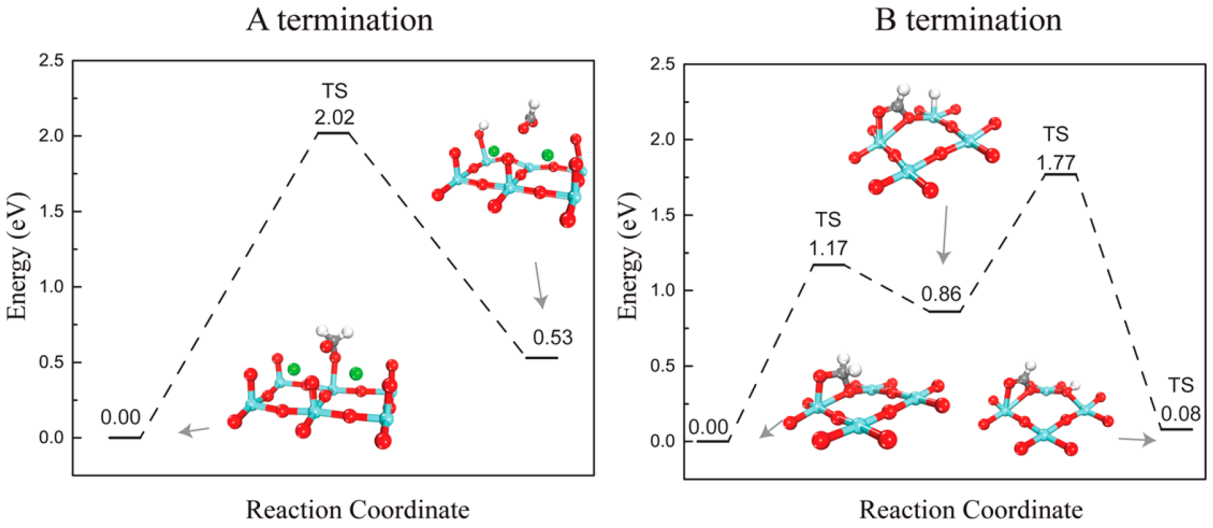

Figure 4. Second C−H bond activation of methoxy groups on $SrTiO_3(100)$ of A termination and B termination. Color code: Sr, green; Ti, cyan; O, red; C, gray; H, white. Only the surface layer is shown.

more energetically favorable than other low-Miller-index surfaces such as (110) and (111).[34,35] Figure 1 shows the structures of the $SrTiO_3(100)$ surface's two terminations: A (SrO) and B (TiO_2). Previous work has reported the formation of surface oxygen vacancies and surface reconstructions of STO surfaces.[36] To provide a baseline understanding, here we consider only the $SrTiO_3(100)$ surface with perfect terminations, leaving the defected and/or reconstructed surfaces for future work. We aim to elucidate the mechanism of methanol coupling, especially the formation of acetate, on the $SrTiO_3(100)$ surface.

3.1. Methanol Adsorption on the $SrTiO_3(100)$ Surface.

Figure 2 shows the structure and energy of methanol adsorption on A and B terminations. One can see that a methanol molecule adsorbs dissociatively on both terminations and a methoxy group thus forms spontaneously. In the A termination, the O−H bond of methanol is cleaved without a barrier and the distance between the O and H is 1.56 Å. The methoxy group adsorbs on the bridge site between two Sr atoms, where the distance between O and Sr is 2.56 Å. On the B termination, the O−H bond is also cleaved spontaneously after adsorption. The methoxy group adsorbs on top of the Ti atom and the H from methanol adsorbs to the nearest lattice oxygen. The calculated adsorption energies, −1.67 and −1.69 eV on the A and B terminations, respectively, suggest that methanol dissociatively adsorbs strongly on both terminations with similar strength.

To simplify the calculations and facilitate the subsequent C−H activation steps, we removed the dissociated surface hydrogen atom after methanol adsorption. To justify our approach, we calculated the migration and desorption of surface hydrogen atoms on the A and B terminations (see Figures S1 and S2 in the Supporting Information). The surface hydrogen atom migrates between neighboring lattice oxygen sites with an energy barrier of 1.87 and 0.35 eV on the A and B terminations, respectively (Figure S1). On the A termination, H desorption to form H_2 is exothermic and requires an activation energy of 1.04 eV; on the B termination, it is slightly endothermic and

DOI: 10.1021/acs.jpcc.8b00273
J. Phys. Chem. C XXXX, XXX, XXX−XXX

requires an activation energy of 1.53 eV (Figure S2). Therefore, one can see that on the A termination H_2 desorption is relatively easy, while on the B termination H migration on the surface is facile and H_2 desorption is not that difficult (if one further factors in entropy gain during desorption).

3.2. C−H Activation of Methoxy. In previous studies of methanol chemistry on metal oxides, it has been found that the coupling reaction is often preceded by activation of C−H bonds of the methoxy group onto the surface.[37,38] We hypothesize that formation of the acetate species from methanol on STO surfaces follows a similar mechanism. To test this idea, we studied the first C−H bond activation of the methoxy group on the STO (100) surface and Figure 3 shows the reaction pathways and the structures along the path.

On both terminations, it is found that the reactions proceed via two steps: CH_3O dehydrogenation and CH_2O oxidation. On the A termination, CH_3O first loses one hydrogen atom to the nearest lattice oxygen atom with an activation energy of 0.29 eV, to produce CH_2O (formaldehyde). In the second step, CH_2O reacts with a surface lattice oxygen via the C atom to form a surface H_2COO_L moiety (O_L denotes a lattice oxygen) where now the C atom becomes sp^3 hybridized. This step is energetically favorable, and the activation energy is only 0.20 eV. On the B termination, the reaction follows a very similar sequence.

We next investigated the second C−H activation, as shown in Figure 4. On the A termination, this process is endothermic and the reaction barrier is predicted to be 2.02 eV, indicating that the second C−H cleavage is unlikely to happen on the A termination. On the B termination, the dehydrogenation process can be divided into two steps: in the first step, the surface H_2COO_L moiety loses one H atom to the Ti top site with an activation energy of 1.17 eV to form $HCOO_L$, a kind of surface formate species; in the second step, the dissociated H atom transfers from Ti to a surface lattice oxygen. One can see from the middle structure in Figure 4B that a hydride (on Ti) intermediate is involved in the process on the B termination, which may be the reason for its lower barrier in the second C−H cleavage.

We further examined the third C−H activation but only on the B termination, since the second C−H bond activation was shown to be very unlikely on the A termination. As shown in Figure 5, the $HCOO_L$ species loses its hydrogen atom to a lattice oxygen with a barrier of 1.66 eV, leading to an adsorbed CO molecule on the surface Ti−O_L pair.

3.3. C−C Coupling Reaction on $SrTiO_3$(100). Since one key goal of the present work is to reveal the mechanism of acetate formation from methanol on $SrTiO_3$(100), we next examined how CH_xO species couple on the surface. Figure 6 shows one of the most likely coupling reactions on the $SrTiO_3$(100) A termination. On the A termination, the coupling reaction occurs between two CH_2O groups, because the formation of CH_2O is facile, but the second C−H cleavage is difficult (Figure 4A). One can see from Figure 6 that, first, one CH_2O group is lifted up from a lattice oxygen site (TS1) and becomes formaldehyde (ii). In other words, the adsorbed CH_2O groups need to be activated from sp^3 to sp^2 hybridization and then they couple together to form ethane-1,2-diolate (OCH_2CH_2O; iii). This process is endothermic, and the activation energy is 1.02 eV (TS2). Then, the OCH_2CH_2O intermediate further dehydrogenates to form an $OCHCH_2O$ intermediate (iv; a deprotonated glycolaldehyde). This step is exothermic with an activation energy of 1.41 eV (TS3). Lastly,

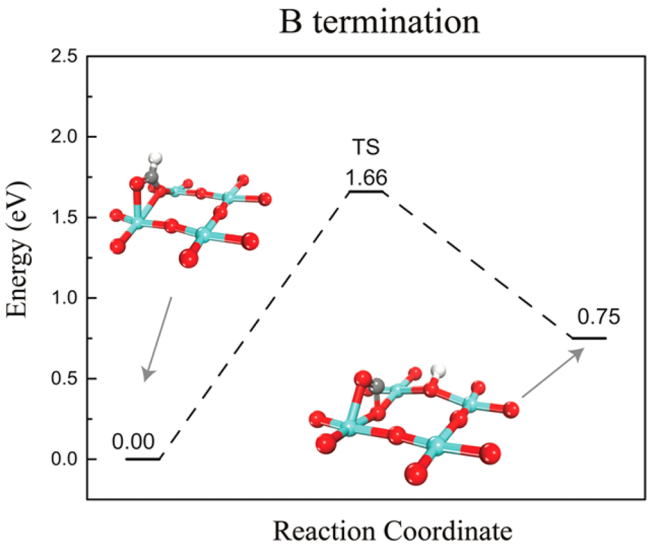

Figure 5. Third C−H bond activation of CH_3O on the $SrTiO_3$(100) B termination. Color code: Ti, cyan; O, red; C, gray; H, white. Only the surface layer is shown.

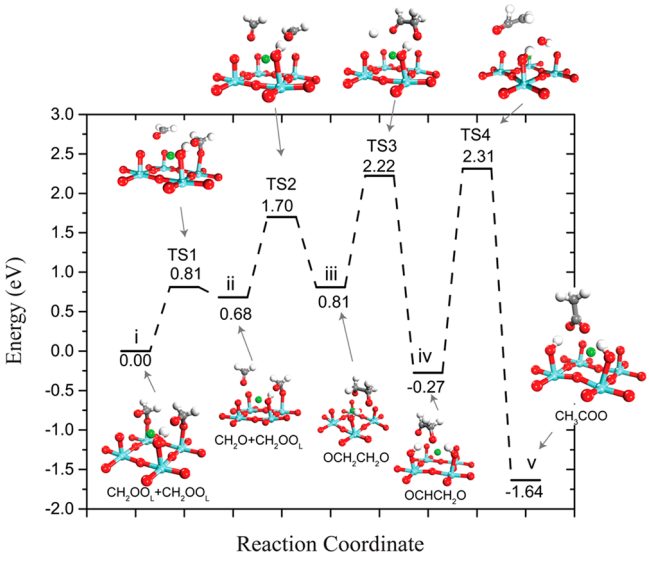

Figure 6. Reaction pathway of C−C coupling between two CH_2O groups on the $SrTiO_3$(100) A termination. Color code: Sr, green; Ti, cyan; O, red; C, gray; H, white. Only the surface layer is shown.

the intermediate $OCHCH_2O$ (iv) reacts to form the adsorbed acetate (CH_3COO; v). This step involves a concerted process of CH_2−O breaking, H transfer between the two C atoms, and formation of a new C−O bond. Although the step is exothermic, it is the rate-limiting step of the whole reaction with an activation barrier of 2.58 eV (TS4), indicating that C−C coupling of methanol on the STO(100) A termination is difficult and that the likely product of coupling on the A termination is $OCHCH_2O$ (Figure 6, iv).

One thing to note is that the STO(100) A termination (i in Figure 6) starts with a hydroxyl group or a preadsorbed H on the surface that could result from dissociative adsorption of methanol (Figure 2). Without this surface hydrogen, we found that OCH_2CH_2O (iii in Figure 6) would dissociate spontaneously. In other words, the surface hydrogen atom can stabilize the intermediate and therefore assist the coupling reaction on the A termination.

DOI: 10.1021/acs.jpcc.8b00273
J. Phys. Chem. C XXXX, XXX, XXX−XXX

Figure 7 shows one of the most likely pathways of the coupling reaction on the $SrTiO_3(100)$ B termination, starting

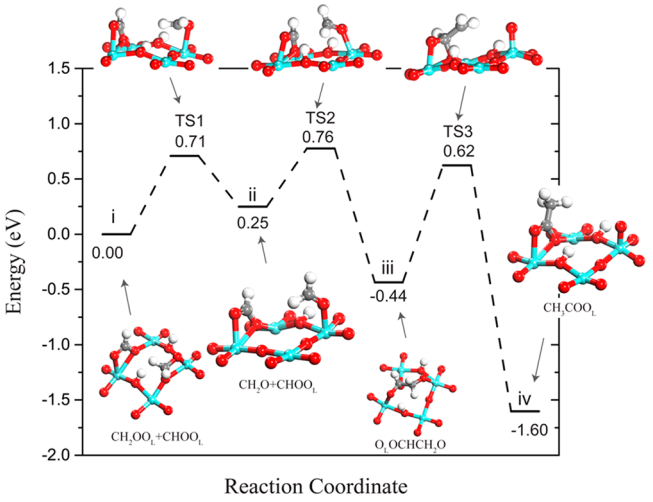

Figure 7. Reaction pathway of C−C coupling between CH_2O and CHO groups on the $SrTiO_3(100)$ B termination. Color code: Ti, cyan; O, red; C, gray; H, white. Only the surface layer is shown.

with one CH_2OO_L and one $CHOO_L$, where L denotes lattice oxygen. We chose these groups as the starting point because their formation is facile (Figures 3B and 4B). The coupling reaction begins with the C−O_L bond breaking in CH_2OO_L (Figure 7, TS1), and then the CH_2O group is lifted up on the surface (ii). It is followed by a direct C−C coupling of the CH_2O and $CHOO_L$ groups, leading to an intermediate state OCH_2CHOO_L (iii). This step is exothermic, and the barrier is predicted to be only 0.51 eV (TS2). Next, the OCH_2CHOO_L intermediate breaks the O−CH_2 bond and the hydrogen atom from the CHO moiety directly transfers to CH_2, forming a methyl group of the surface acetate. This step is exothermic and the barrier is predicted to be 1.06 eV (TS3), leading to formation of CH_3COO_L, an acetate species on the surface (iv). Figure 7 shows that surface acetate formation is more facile on the B termination than on the A termination of $SrTiO_3(100)$.

We note that the STO(100) B termination (i in Figure 7) also starts with a hydroxyl group or a preadsorbed hydrogen atom on the surface. To reveal its role here, we compared the energetics of the critical elementary steps (ii → iii → iv) with and without a surface hydrogen atom (Figure S3). We found that the presence of the surface hydrogen not only stabilizes the intermediate iii but also lowers the activation energy of the acetate formation (iii → iv in Figure 7). This may be due to the surface metallization induced by the hydrogen atom. On both terminations, it has been reported that the surface hydrogen can donate electrons to the surface band, leading to surface metallization.[39] More recently, photoemission spectroscopy and transport measurements confirmed the metallic state.[40]

We have also considered acetate formation from the self-coupling of CH_2O and CHO on the B termination. For CH_2O (Figure S4), the two CH_2O groups first form an OCH_2CH_2O intermediate; next, OCH_2CH_2O dehydrogenates to form an OCH_2CHO intermediate; then, OCH_2CHO coverts an acetate species. The last step requires a high activation energy of 2.87 eV. For CHO (Figure S5), the acetate formation step also requires a high activation energy of 2.83 eV. In contrast, the acetate formation step in the heterocoupling of CH_2O and CHO as shown in Figure 7 has a much lower barrier (1.06 eV).

3.4. Comparison with the Experimental Data. Temperature-programmed desorption (TPD) of methanol from the single-crystal $SrTiO_3(100)$ surface found that a small amount of formaldehyde desorbs from the surface below 100 °C.[25] This observation is in agreement with our finding that methoxy formation and its first dehydrogenation to form CH_2O is facile on both terminations of $SrTiO_3(100)$. Ambient-pressure XPS (APXPS) spectra of 0.1 Torr of methanol on $SrTiO_3(100)$ at a surface temperature of 250 °C (Figure 8) showed formation of

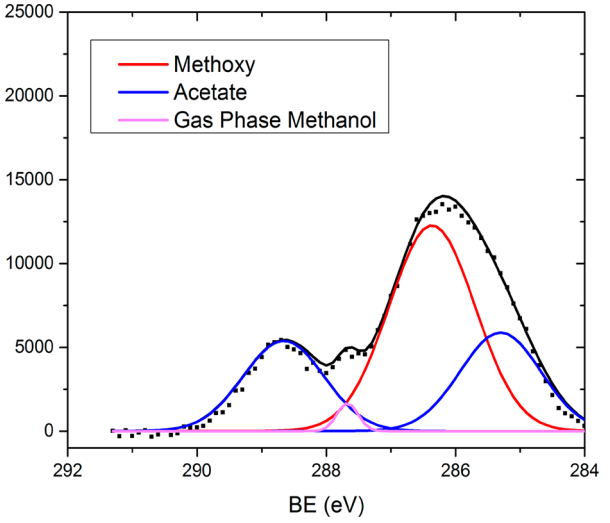

Figure 8. C 1s ambient-pressure XPS (APXPS) spectrum (dotted line) of a $SrTiO_3(100)$ surface at 250 °C after the addition of 0.1 Torr of methanol. The total fitted spectrum (black line) is from summing up the contributions from acetate (blue line), methoxy (red line), and gas-phase methanol (pink line).

methoxy and acetate on the surface, accompanied by reduction of surface Ti. Although the acetate formation came as a surprise from the APXPS spectra, our mechanistic studies here show that it is indeed possible, especially on the B termination. This is in agreement with the experimental observation that the $SrTiO_3(100)$ surface tends to expose the B termination after annealing in O_2,[41] as done in our sample in Figure 8.

4. SUMMARY AND CONCLUSIONS

We have studied methanol coupling on $SrTiO_3$ surfaces to form adsorbed acetate by density functional theory. The A and B terminations of a perfect (100) surface were examined. Methanol molecules were found to adsorb dissociatively on both A and B terminations with similar adsorption energies. C−C coupling reactions were found to be preceded by C−H activation of CH_3O. Although the first dehydrogenation step to form CH_2O on the surface was found to be facile on both $SrTiO_3(100)$ terminations (activation energy <0.5 eV), the second dehydrogenation to form CHO on the surface was found to be much more difficult on the A termination (activation energy >2.0 eV). Hence, the coupling reaction was considered to take place between two adsorbed CH_2O groups on the A termination, while the coupling between CH_2O and CHO was found to be most likely on the B termination. Examination of the most likely coupling pathways indicates that formation of adsorbed acetate on the A termination is much more difficult (activation energy of the most difficult step >2.5

DOI: 10.1021/acs.jpcc.8b00273
J. Phys. Chem. C XXXX, XXX, XXX−XXX

eV) than on the B termination. This work suggests that, for the C−C coupling reaction of oxygenates on perovskites, a B termination is most beneficial. The computational results can well explain the ambient-pressure XPS spectrum of methanol on single-crystal $SrTiO_3$(100).

■ ASSOCIATED CONTENT

Supporting Information

The Supporting Information is available free of charge on the ACS Publications website at DOI: 10.1021/acs.jpcc.8b00273.

Hydrogen diffusion and desorption pathways; impact of surface hydrogen on energetics; and self-coupling of CH_2O and CHO groups on the $SrTiO_3$(100) B termination (PDF)

■ AUTHOR INFORMATION

Corresponding Author

*E-mail: djiang@ucr.edu.

ORCID

Victor Fung: 0000-0002-3347-6983
David R. Mullins: 0000-0003-3495-7188
Zili Wu: 0000-0002-4468-3240
De-en Jiang: 0000-0001-5167-0731

Notes

The authors declare no competing financial interest.

■ ACKNOWLEDGMENTS

This research is sponsored by the U.S. Department of Energy, Office of Science, Office of Basic Energy Sciences, Chemical Sciences, Geosciences, and Biosciences Division. This research used resources of the National Energy Research Scientific Computing Center, a DOE Office of Science User Facility supported by the Office of Science of the U.S. Department of Energy under Contract No. DE-AC02-05CH11231. APXPS spectra were recorded at Beamline 23-ID-2 of the National Synchrotron Light Source II, a U.S. Department of Energy (DOE) Office of Science User Facility operated for the DOE Office of Science by Brookhaven National Laboratory under Contract No. DE-SC0012704.

■ REFERENCES

(1) Schwach, P.; Pan, X.; Bao, X. Direct Conversion of Methane to Value-Added Chemicals over Heterogeneous Catalysts: Challenges and Prospects. *Chem. Rev.* **2017**, *117*, 8497−8520.

(2) Bjørgen, M.; Joensen, F.; Holm, M. S.; Olsbye, U.; Lillerud, K.-P.; Svelle, S. Methanol to Gasoline over Zeolite H-ZSM-5: Improved Catalyst Performance by Treatment with NaOH. *Appl. Catal., A* **2008**, *345*, 43−50.

(3) Chang, C. D.; Chu, C. T.; Socha, R. F. Methanol Conversion to Olefins over ZSM-5: I. Effect of Temperature and Zeolite $SiO_2Al_2O_3$. *J. Catal.* **1984**, *86*, 289−296.

(4) Wittstock, A.; Zielasek, V.; Biener, J.; Friend, C. M.; Bäumer, M. Nanoporous Gold Catalysts for Selective Gas-Phase Oxidative Coupling of Methanol at Low Temperature. *Science (Washington, DC, U. S.)* **2010**, *327*, 319−322.

(5) McCann, D. M.; Lesthaeghe, D.; Kletnieks, P. W.; Guenther, D. R.; Hayman, M. J.; Van Speybroeck, V.; Waroquier, M.; Haw, J. F. A Complete Catalytic Cycle for Supramolecular Methanol-to-Olefins Conversion by Linking Theory with Experiment. *Angew. Chem.* **2008**, *120*, 5257−5260.

(6) Dessau, R. On the H-ZSM-5 Catalyzed Formation of Ethylene from Methanol or Higher Olefins. *J. Catal.* **1986**, *99*, 111−116.

(7) Goguen, P. W.; Xu, T.; Barich, D. H.; Skloss, T. W.; Song, W.; Wang, Z.; Nicholas, J. B.; Haw, J. F. Pulse-quench Catalytic Reactor Studies Reveal a Carbon-Pool Mechanism in Methanol-to-Gasoline Chemistry on Zeolite H-ZSM-5. *J. Am. Chem. Soc.* **1998**, *120*, 2650−2651.

(8) Zaidi, H.; Pant, K. Catalytic Conversion of Methanol to Gasoline Range Hydrocarbons. *Catal. Today* **2004**, *96*, 155−160.

(9) Svelle, S.; Joensen, F.; Nerlov, J.; Olsbye, U.; Lillerud, K.-P.; Kolboe, S.; Bjørgen, M. Conversion of Methanol into Hydrocarbons Over Zeolite H-ZSM-5: Ethene Formation is Mechanistically Separated from the Formation of Higher Alkenes. *J. Am. Chem. Soc.* **2006**, *128*, 14770−14771.

(10) Bjørgen, M.; Svelle, S.; Joensen, F.; Nerlov, J.; Kolboe, S.; Bonino, F.; Palumbo, L.; Bordiga, S.; Olsbye, U. Conversion of Methanol to Hydrocarbons Over Zeolite H-ZSM-5: On the Origin of the Olefinic Species. *J. Catal.* **2007**, *249*, 195−207.

(11) Bjørgen, M.; Olsbye, U.; Petersen, D.; Kolboe, S. The Methanol-to-hydrocarbons Reaction: Insight into the Reaction Mechanism from [^{12}C] Benzene and [^{13}C] Methanol Coreactions over Zeolite H-beta. *J. Catal.* **2004**, *221*, 1−10.

(12) Scheuermann, G. M.; Rumi, L.; Steurer, P.; Bannwarth, W.; Mülhaupt, R. Palladium Nanoparticles on Graphite Oxide and its Functionalized Graphene Derivatives as Highly Active Catalysts for the Suzuki−Miyaura Coupling Reaction. *J. Am. Chem. Soc.* **2009**, *131*, 8262−8270.

(13) *Metal-Catalyzed Cross-Coupling Reactions*; Diederich, F.; Stang, P. J., Eds., Wiley-VCH: Weinheim, 1998.

(14) Dyker, G. Transition Metal Catalyzed Coupling Reactions under C−H Activation. *Angew. Chem., Int. Ed.* **1999**, *38*, 1698−1712.

(15) Yin, L.; Liebscher, J. Carbon−Carbon Coupling Reactions Catalyzed by Heterogeneous Palladium Catalysts. *Chem. Rev.* **2007**, *107*, 133−173.

(16) Zhu, H.; Zhang, P.; Dai, S. Recent Advances of Lanthanum-based Perovskite Oxides for Catalysis. *ACS Catal.* **2015**, *5*, 6370−6385.

(17) Royer, S.; Duprez, D.; Can, F.; Courtois, X.; Batiot-Dupeyrat, C.; Laassiri, S.; Alamdari, H. Perovskites as Substitutes of Noble Metals for Heterogeneous Catalysis: Dream or Reality. *Chem. Rev.* **2014**, *114*, 10292−10368.

(18) Pena, M.; Fierro, J. Chemical Structures and Performance of Perovskite Oxides. *Chem. Rev.* **2001**, *101*, 1981−2018.

(19) Foo, G. S.; Polo Garzon, F.; Fung, V.; Jiang, D.; Overbury, S. H.; Wu, Z. Acid-Base Reactivity of Perovskite Catalysts Probed via Conversion of 2-Propanol Over Titanates and Zirconates. *ACS Catal.* **2017**, *7*, 4423−4434.

(20) Kim, C. H.; Qi, G.; Dahlberg, K.; Li, W. Strontium-Doped Perovskites Rival Platinum Catalysts for Treating NO_X in Simulated Diesel Exhaust. *Science (Washington, DC, U. S.)* **2010**, *327*, 1624−1627.

(21) Yamazoe, N.; Teraoka, Y. Oxidation Catalysis of Perovskites-Relationships to Bulk Structure and Composition (valency, defect, etc.). *Catal. Today* **1990**, *8*, 175−199.

(22) Borchert, H.; Baerns, M. The Effect of Oxygen-Anion Conductivity of Metal−Oxide Doped Lanthanum Oxide Catalysts on Hydrocarbon Selectivity in the Oxidative Coupling of Methane. *J. Catal.* **1997**, *168*, 315−320.

(23) Imai, H.; Tagawa, T.; Kamide, N. Oxidative Coupling of Methane over Amorphous Lanthanum Aluminum Oxides. *J. Catal.* **1987**, *106*, 394−400.

(24) Spinicci, R.; Marini, P.; De Rossi, S.; Faticanti, M.; Porta, P. Oxidative Coupling of Methane on $LaAlO_3$ Perovskites Partially Substituted with Alkali or Alkali-earth Ions. *J. Mol. Catal. A: Chem.* **2001**, *176*, 253−265.

(25) Zhang, Y.; Savara, A.; Mullins, D. R. Ambient-Pressure XPS Studies of Reactions of Alcohols on $SrTiO_3$(100). *J. Phys. Chem. C* **2017**, *121*, 23436−23445.

(26) Kresse, G.; Furthmüller, J. Efficiency of Ab-initio Total Energy Calculations for Metals and Semiconductors using a Plane-Wave Basis Set. *Comput. Mater. Sci.* **1996**, *6*, 15−50.

(27) Perdew, J. P.; Burke, K.; Ernzerhof, M. Generalized Gradient Approximation Made Simple. *Phys. Rev. Lett.* **1996**, *77*, 3865−3868.

DOI: 10.1021/acs.jpcc.8b00273
J. Phys. Chem. C XXXX, XXX, XXX−XXX

(28) Kresse, G.; Joubert, D. From Ultrasoft Pseudopotentials to the Projector Augmented-Wave Method. *Phys. Rev. B: Condens. Matter Mater. Phys.* **1999**, *59*, 1758−1775.
(29) Blöchl, P. E. Projector Augmented-Wave Method. *Phys. Rev. B: Condens. Matter Mater. Phys.* **1994**, *50*, 17953−17979.
(30) Lytle, F. W. X-Ray Diffractometry of Low-Temperature Phase Transformations in Strontium Titanate. *J. Appl. Phys.* **1964**, *35*, 2212−2215.
(31) Grimme, S.; Antony, J.; Ehrlich, S.; Krieg, H. A Consistent and Accurate Ab Initio Parametrization of Density Functional Dispersion Correction (DFT-D) for the 94 Elements H-Pu. *J. Chem. Phys.* **2010**, *132*, 154104.
(32) Henkelman, G.; Uberuaga, B. P.; Jónsson, H. A Climbing Image Nudged Elastic Band Method for Finding Saddle Points and Minimum Energy Paths. *J. Chem. Phys.* **2000**, *113*, 9901−9904.
(33) Henkelman, G.; Jónsson, H. Improved Tangent Estimate in the Nudged Elastic Band Method for Finding Minimum Energy Paths and Saddle Points. *J. Chem. Phys.* **2000**, *113*, 9978−9985.
(34) Bottin, F.; Finocchi, F.; Noguera, C. Stability and Electronic Structure of the (1 × 1) $SrTiO_3$ Polar Surfaces by First-Principles Calculations. *Phys. Rev. B: Condens. Matter Mater. Phys.* **2003**, *68*, 035418.
(35) Woo, S.; Jeong, H.; Lee, S. A.; Seo, H.; Lacotte, M.; David, A.; Kim, H. Y.; Prellier, W.; Kim, Y.; Choi, W. S. Surface Properties of Atomically Flat Poly-Crystalline $SrTiO_3$. *Sci. Rep.* **2015**, *5*, 8822.
(36) Stashans, A.; Erazo, F.; Ortiz, J.; Valverde, P. Oxygen-vacancy Defects on the $SrTiO_3$ (001) Surface: a Quantum-Chemical Study. *Philos. Mag. B* **2001**, *81*, 1977−1988.
(37) Xu, B.; Liu, X.; Haubrich, J.; Madix, R. J.; Friend, C. M. Selectivity Control in Gold-Mediated Esterification of Methanol. *Angew. Chem., Int. Ed.* **2009**, *48*, 4206−4209.
(38) Xu, B.; Haubrich, J.; Baker, T. A.; Kaxiras, E.; Friend, C. M. Theoretical Study of O-Assisted Selective Coupling of Methanol on Au(111). *J. Phys. Chem. C* **2011**, *115*, 3703−3708.
(39) Lin, F.; Wang, S.; Zheng, F.; Zhou, G.; Wu, J.; Gu, B.-L.; Duan, W. Hydrogen-induced metallicity of $SrTiO_3$ (001) surfaces: A Density Functional Theory Study. *Phys. Rev. B: Condens. Matter Mater. Phys.* **2009**, *79*, 035311.
(40) D'Angelo, M.; Yukawa, R.; Ozawa, K.; Yamamoto, S.; Hirahara, T.; Hasegawa, S.; Silly, M. G.; Sirotti, F.; Matsuda, I. Hydrogen-Induced Surface Metallization of $SrTiO_3$(001). *Phys. Rev. Lett.* **2012**, *108*, 116802.
(41) Dagdeviren, O. E.; Simon, G. H.; Zou, K.; Walker, F. J.; Ahn, C.; Altman, E. I.; Schwarz, U. D. Surface Phase, Morphology, and Charge Distribution Transitions on Vacuum and Ambient Annealed $SrTiO_3$(100). *Phys. Rev. B: Condens. Matter Mater. Phys.* **2016**, *93*, 195303.

DOI: 10.1021/acs.jpcc.8b00273
J. Phys. Chem. C XXXX, XXX, XXX−XXX